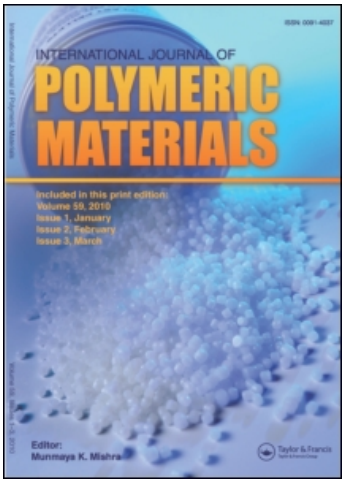

International Journal of Polymeric Materials
Publication details, including instructions for authors and subscription information:
http://www.informaworld.com/smpp/title~content=t713647664

Dynamic Mechanical Properties of Block Copolymer Blends—A Study of the Effects of Terminal Chains in Elastomeric Materials

R. E. Cohen[a]; N. W. Tschoegl[b]
[a] Department of Chemical Engineering, Massachusetts Institute of Technology, Cambridge, Mass [b] Division of Chemistry and Chemical Engineering, California Institute of Technology Pasadena, California

To cite this Article Cohen, R. E. and Tschoegl, N. W.(1974) 'Dynamic Mechanical Properties of Block Copolymer Blends—A Study of the Effects of Terminal Chains in Elastomeric Materials', International Journal of Polymeric Materials, 3: 1, 3 — 22
To link to this Article: DOI: 10.1080/00914037408072371
URL: http://dx.doi.org/10.1080/00914037408072371

Intern. J. Polymeric Mater., 1974, Vol. 3, pp. 3–22

Printed in Reading, England

Dynamic Mechanical Properties of Block Copolymer Blends—A Study of the Effects of Terminal Chains in Elastomeric Materials

3. A Mathematical Model for Entanglement Slippage

R. E. COHEN † and N. W. TSCHOEGL

Division of Chemistry and Chemical Engineering, California Institute of Technology Pasadena, California 91109

(*Received March 9, 1973*)

A mathematical model is presented which describes the phenomenon of entanglement slippage in elastomeric triblock–diblock copolymer blends. Three separate mechanisms, representing the slippage of entanglements between triblock center segments, between center segments and terminal chains, and between terminal chains alone, are incorporated into the model. The contribution of each mechanism to the overall material behavior is calculated on the basis of the concentration and length of the terminal chains in the entanglement network. Predictions of the model compare favorably with previously reported measurements of the mechanical properties of a series of block copolymer blends.

INTRODUCTION

The first paper of this series[1] introduced the use of block copolymer blends as model materials for the study of molecular motions in elastomers. It was shown[1,2] that blends of polystyrene-1,4-polybutadiene (SB) diblocks and polybutadiene continuous SBS triblocks can be used advantageously to elucidate the effects of terminal chains and of chain entanglements on the dynamic mechanical behavior of rubbers.

Free oscillation (isochronal) measurements[1] conducted on three series of SB–SBS blends provided qualitative evidence that, in addition to their role as

†Present address: Department of Chemical Engineering, Massachusetts Institute of Technology, Cambridge, Mass.

internal plasticizers, terminal chains can take part in secondary viscoelastic mechanisms having relaxation times which are large compared to those associated with the polybutadiene glass transition. Forced oscillation (isothermal) measurements[2] revealed significant low frequency losses in all the materials studied. Both the magnitude and the location of the low frequency losses along the logarithmic frequency scale were greatly affected by changes in network composition. No quantitative interpretation of these phenomena was given in the earlier papers. In this paper we examine the low frequency processes and develop a mathematical model for the quantitative description of entanglement slippage.

ENTANGLEMENT SLIPPAGE IN BLOCK COPOLYMER BLENDS

The rubbery networks of our block copolymer blends are held together only by the glassy crosslinks provided by the rigid polystyrene domains; no covalent crosslinks are present. Furthermore, the polystyrene domains are relatively large and immobile. Thus contributions to the low frequency losses from motions of the permanent network linkage points can be ignored here. This was not the case in earlier studies of entanglements in rubbers[3–10] where entanglement slippage effects were overlapped by the influence of changing crosslink density. Our model networks contain a controlled combination[1] of permanent (or trapped) and non-permanent (or untrapped) entanglements. The former arise from entanglements between two triblock polybutadiene segments; the latter are formed either by the entanglement of two diblock segments or by the entanglement of a diblock and a triblock segment.

At sufficiently low reduced frequencies long polybutadiene segments will have time to slip past each other during a cyclic deformation. These motions are not sufficient to enable trapped entanglements to disengage since all chains eventually end in glassy domains. However, the positions of the trapped entanglements will change continuously as the network seeks to accommodate imposed stresses or strains. Thus, vibrational sliding motions occur at low frequencies in the trapped entanglement portion of the network. The characteristic distances for these sliding motions will depend upon network composition. As the network becomes looser with increasing terminal chain content the average distance between trapped entanglements, and therefore the retardation times associated with the trapped entanglement slippage process, increases.

The untrapped entanglements can completely disentangle through these motions and, therefore, allow very long range slippage. The characteristic distances for the slippage of untrapped entanglements will depend upon the type of untrapped entanglement involved (between terminal chains or between terminal chains and center blocks) and upon the length and concentration of

terminal chains in the network. The mobility of the free ends associated with untrapped entanglements suggests that longer range disentangling motions may be favored over the kind of shorter range sliding motions identified with trapped entanglements. Thus we may well expect the mechanisms associated with untrapped entanglement slippage to be weighted more heavily toward long time processes.

At equilibrium all of the untrapped entanglements will be disentangled. The compliance will have risen from a temporary plateau, reflecting the contributions of all types of entanglement,[11] to a final equilibrium level to which only trapped entanglements contribute. It is the nature of the viscoelastic transition between these two levels which we examine here. We will present information concerning the mechanisms of entanglement slippage through modelling of the shape and location of this transition.

PARAMETERS OF THE MATHEMATICAL MODEL

The model is presented in terms of parameters which may easily be determined. The most important parameters are:

- M_e —molecular weight between entanglements; for our network systems $M_e = 13{,}000$ as determined by swelling measurements.[1]
- M' —terminal chain molecular weights; 67,000, 51,000 and 22,000 in the three series of specimens already studied.
- M —molecular weight of rubbery chains in the network; this corresponds to the 78,000 molecular weight of the polybutadiene segment of the triblock material.
- X —weight fraction of terminal chains in the polybutadiene phase of the diblock–triblock blends.

The mathematical model to be developed is not a molecular theory for chain entanglements. Such theories have been the object of many investigations. The degree of success and applicability of the theories have been summarized.[11] The theories are generally formulated in terms of a spectrum of relaxation or retardation times from which the overall material response can be calculated. Although the low frequency response associated with entanglement slippage can often be predicted adequately in this manner, there is generally no information on the individual viscoelastic mechanisms which make up the spectrum. In the approach presented in this paper the contributions of each mechanism is estimated from the experimental data. The spectrum is then modified by appropriately weighting the various separate contributions and by changing the location of the contribution of each mechanism along the frequency scale. These changes in weighting and location will be described, through the model to be developed, in terms of the parameters listed above.

THE MODEL

A generalized Voigt model is often used to represent the linear viscoelastic behavior of polymers. The appropriate expressions for the storage and loss compliances are

$$D'(\omega) = D_g + \sum_i D_i/(1 + \omega^2\tau_i^2) \tag{1}$$

$$D''(\omega) = \sum_i D_i\omega\tau_i/(1 + \omega^2\tau_i^2) \tag{2}$$

In these expressions the summation over i accounts for a distribution of retardation times, τ_i, with associated retardation strength, D_i. Alternatively, the retardation strength can be envisioned as resulting from a total of D_i distinct retardation times, all of unit retardation strength, superposing at $\omega = 1/\tau_i$ on the frequency scale. In this sense we may call D_i the degeneracy of τ_i. The constant D_g appearing in Eq. (1) represents the glassy compliance of the material. The value of D_g is roughly the same for a wide variety of polymers, and, except at the very highest frequencies of interest, it is entirely negligible in comparison with the sum over i.

A simple modification of the generalized Voigt model, allowing for the possibility of several distributed viscoelastic mechanisms each with its own spectrum of retardation times, results in the following expressions for the storage and loss compliances:

$$D'(\omega) = D_g + \sum_{k=1}^{n} \sum_{i=1}^{nk} D_{ik}/(1 + \omega^2\tau_{ik}^2) \tag{3}$$

$$D''(\omega) = \sum_{k=1}^{n} \sum_{i=1}^{nk} D_{ik}\omega\tau_{ik}/(1 + \omega^2\tau_{ik}^2) \tag{4}$$

The value of the index k indicates which of the n contributing viscoelastic mechanisms is being considered. Each will have a different set of retardation times, a total of n_k values of τ_{ik} for the kth mechanism. The D_{ik} values represent the spectral strength associated with each τ_{ik}.

Equations (3) and (4) are formally equivalent to the transient network model of Lodge,[13] but the interpretation of the parameters on the molecular level is different. The expressions represent the addition of several groups of Voigt elements whose contributions appear clustered at various positions along the frequency scale. In this sense Eqs. (3) and (4) can be considered as a generalization of the more restricted model for the behavior of entangled polymers proposed by Ferry and coworkers in which $n = 2$.[14]

If left completely unrestricted in terms of the choices of the number of mechanisms, n, and the various τ's and D's, for each mechanism, Eqs. (3) and

(4) could be made to fit nearly any observed response. They thus represent a convenient starting point from which to build a model. The choices will not be arbitrary, however, but will be dictated by the molecular structure of the network under consideration.

The parameter to be determined first is n, the number of viscoelastic mechanisms contributing to the mechanical response. For the triblock, containing no terminal chains, it is easily seen from the data[1,2] that $n = 2$ is the appropriate value, $k = 1$ corresponding to the main transition and $k = 2$ accounting for the slippage of trapped entanglements. Our model is not expected to account for contributions from an interlayer[12,15–17] or from the polystyrene phase[15,18,19] because it is concerned with the behavior of the polybutadiene phase only.

For the diblock–triblock blends $n = 4$ with $k = 1$ and $k = 2$ being as before, and, in addition, $k = 3$ corresponding to the slippage of untrapped entanglements between terminal chains and center blocks, and $k = 4$ accounting for the slippage of untrapped entanglements between terminal chains only. Each of these mechanisms must be identified with a certain spectrum of retardation times distributed along the time or frequency scale.

We begin by considering that, at very low frequencies, each of the viscoelastic mechanisms will have contributed its entire effect and the storage compliance will have reached the equilibrium value, D_e. This is the sum of the individual contributions from each of the four mechanisms listed above. Thus, at very low frequencies we have

$$\sum_{k=1}^{4} \sum_{i=1}^{nk} D_{ik} = D_e - D_g \cong D_e \tag{5}$$

where, as indicated earlier, the glassy compliance can be neglected. Equation (5) simply states that D_e is the sum of the degeneracies of all the retardation times of unit retardation strength. It does not indicate how these are distributed among the individual mechanisms. As is well known, however, we can determine a numerical value of D_e by replacing the summation in Eq. (5) by an integration, i.e. by integrating over the entire retardation spectrum.

We first evaluate the equilibrium compliances of the SBS-8 triblock, designating it as $D_e{}^t$. Figure 1 shows the retardation spectra for the SBS-8 triblock and one of the blends, BL-1.3, in the customary doubly logarithmic plot. This blend contained 0.577% of terminal chains of molecular weight 51,000 in the polybutadiene phase. The spectra were calculated by the approximation methods of Tschoegl,[20] and the symbol $L_2''(\tau)$ indicates that the second central approximation based on loss compliance data has been employed. In Figure 2 the retardation spectrum for SBS-8 is replotted with a linear ordinate. The peak at the lower frequencies corresponds to the main transition ($k = 1$), and that at the higher frequencies to the slippage of trapped entanglements ($k = 2$).

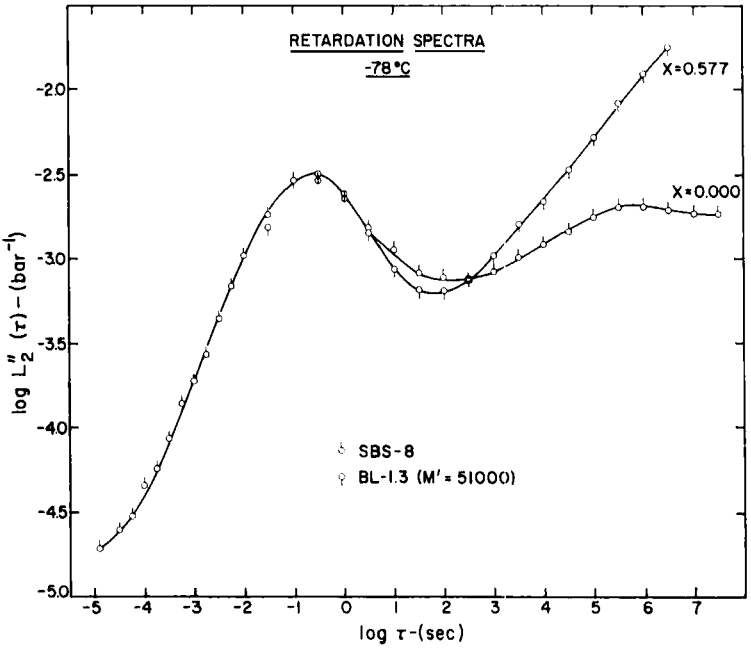

FIGURE 1 Logarithmic plots of the retardation spectra for SBS-8 and BL-1.3.

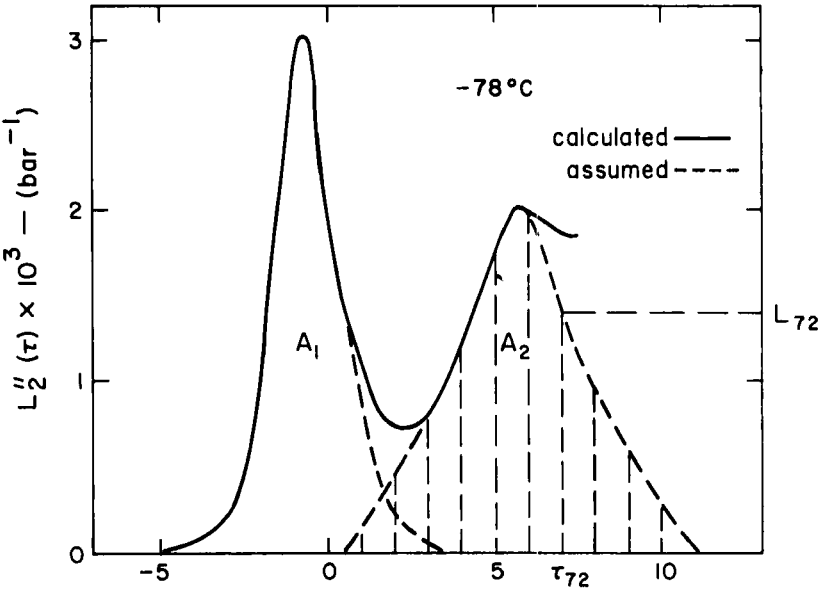

FIGURE 2 Linear plot of the retardation spectrum for SBS-8.

The right side of the secondary peak has been assumed to be symmetric with its left side on the logarithmic scale of retardation times. The apparent persistence of the calculated spectrum at long times above the assumed shape may be explained, at least partially, by the onset of contributions from an interlayer or from the polystyrene phase.[12,15-19] The validity of the symmetry assumption cannot be proven; this simply represents a reasonable way to estimate the total long-time contribution to the equilibrium compliance. The resulting value for D_e^t is $10^{-1.84}$ bar^{-1} (1 bar equals 10^6 dynes/cm^2 or 14.5 psi).

Figure 2 allows the total number of retardation times of unit retardation strength to be split into the two fractions Z_t (associated with $k = 1$) and $1 - Z_t$ (associated with $k = 2$). The numerical value of Z_t is determined as the ratio of the area under the main peak to the total area, or

$$Z_t = A_1/(A_1 + A_2) \tag{6}$$

where the A's represent the areas shown in Figure 2. This results in a value of 0.419 for Z_t. For $1 - Z_t$ we have, similarly,

$$1 - Z_t = A_2/(A_1 + A_2) \tag{7}$$

the numerical value of the fraction being 0.581.

Since D_e^t may be regarded as the sum of the degeneracies of all retardation times of unit retardation strength, we thus find that in the triblock there are $D_e^t Z_t$ such retardation times associated with the main transition and $D_e^t(1 - Z_t)$ with the slippage of trapped entanglements. Since we know the distribution of these times from Figure 2, we should be able to reproduce the experimentally observed response by calculation. This is accomplished by collocating values of the spectral strength L_{ik} to approximately chosen values of τ_{ik}, as illustrated schematically in Figure 2 for τ_{72} and calculating the retardation strengths to be inserted into Eqs. (3) and (4) from the relations

$$D_{i1} = D_e^t Z_t \left(L_{i1} / \sum_{i=1}^{n1} L_{i1} \right) \tag{8}$$

and

$$D_{i2} = D_e^t (1 - Z_t) \left(L_{i2} / \sum_{i=1}^{n2} L_{i2} \right) \tag{9}$$

where the division of each L_{ik} by the summation constitutes a normalization of the area under each peak to unity. Since

$$\sum_{i=1}^{nk} L_{ik} = A_k \tag{10}$$

We may, using Eqs. (6) and (7), also write

$$D_{i1} = (D_e{}^t/A)L_{i1} \tag{11}$$

and

$$D_{i2} = (D_e{}^t/A)L_{i2} \tag{12}$$

where $A = A_1 + A_2$ is the total area under the two peaks. The choice of the spacing of the τ_{ik}'s is unimportant as long as they are close enough to yield smooth curves.[12] In practice, a spacing of 0.25 logarithmic units was used. This resulted in values for n_k of 34 for $k = 1$, and 43 for $k = 2$. The procedure ensures that the total number of retardation times of unit retardation strength is always equal to $D_e{}^t$. The response curves calculated in this manner for the SBS-8 triblock are compared with the experimental ones in Figures 6, 7, and 8 where the symbol A refers to the triblock. The agreement is excellent.

Determination of $D_e{}^t$ and Z_t has provided us with two parameters which we may use to advantage in treating the triblock–diblock blends. $D_e{}^t$ essentially represents a scale factor which assures that the calculated response curves will appear at the same numerical level as the experimentally observed behavior. Indeed, the entire scheme could be made dimensionless by dividing observed data and both sides of Eqs. (3) and (4) by $D_e{}^t$. The second parameter, Z_t, simply assigns the appropriate number of unit strength retardation times to the main transition. With the help of $D_e{}^t$ and Z_t it is now possible to determine the model parameters corresponding to a general diblock–triblock blend containing a weight fraction X of terminal chains of molecular weight M'. Based on the results of earlier investigations of the effects of terminal chains in conventional elastomers,[21,22] we should expect the addition of terminal chains to increase the equilibrium compliance from $D_e{}^t$ to a larger value, say $D_e(X)$. We write the symbol for the equilibrium compliances of blends in this way to emphasize their dependence on the terminal chain content, X. Thus we may write

$$D_e(X) = D_e{}^t/f(X) \tag{13}$$

where $D_e(X)$ is the total number of unit strength retardation times in a given blend. The undetermined function $f(X)$ represents the fraction of all the network junctions which are effective[21] at equilibrium. In our case this is simply the fraction of trapped entanglements. An explicit expression for $f(X)$ will be developed presently.

A second relation is obtained from the observations, demonstrated in the earlier two papers of this series, that the presence of terminal chains does not effect either the shape or the location on the logarithmic frequency axis of the main transition. Thus $D_e{}^t Z_t$ must be constant for the triblock and all blends. We can express this by writing

$$D_e(X)Z(X) = D_e{}^t Z_t \tag{14}$$

where $Z(X)$, the fraction of retardation times of unit retardation strength in each blend associated with the main transition, is an adjustable parameter which assures that the response curves calculated from the model will all be identical in the region of the main transition. We recognize that the model defines the main transition by curve fitting to agree with experimental observation, and therefore cannot generate any useful information concerning the behavior of the materials in the transition region.

Equations (13) and (14) define for any blend the total number of retardation times, $D_e(X)$, and the fraction of these, $Z(X)$, which are associated with the main transition. This leaves a fraction $1 - Z(X)$ of the total number of retardation times to be distributed among the three remaining mechanisms. This breakdown can be handled in terms of network parameters if two assumptions are made. First, it is necessary to assume[1,12] that diblock and triblock polybutadiene segments have the same characteristic entanglement length. Second, it must be assumed that each type of entanglement contributes to the frequency dependent mechanical behavior in such a way that the number of unit strength retardation times attributed to each of the three entanglement slippage mechanisms ($k = 2, 3, 4$) will be proportional to the probability of finding each type of entanglement in the network.

The probabilities of finding a diblock segment or a triblock segment at some point in the polybutadiene phase are the weight fractions X and $1 - X$ respectively. Under the first assumption above, the probabilities that a diblock or a triblock segment will enter into some kind of entanglement are also equal to X and $1 - X$ respectively. Then the probability of finding two triblock segments at the same point, i.e. the probability of finding a trapped entanglement, is given by the expression $(1 - X)^2$. Similarly, an untrapped entanglement between two diblock segments would be expected to occur with probability X^2. Untrapped entanglements between a diblock and a triblock segment involve two possibilities, since chain A may originate from a diblock segment and chain B from a triblock segment, or vice versa. Thus a factor of two enters the expression $2X(1 - X)$ which is the probability of finding an untrapped entanglement between a diblock and a triblock segment. In summary:

$$\begin{aligned} p(k = 2) &= p\text{ (triblock–triblock entanglement)} = (1 - X)^2 \\ p(k = 3) &= p\text{ (diblock–triblock entanglement)} = 2X(1 - X) \\ p(k = 4) &= p\text{ (diblock–diblock entanglement)} = X^2 \end{aligned} \tag{15}$$

where

$$\sum_{k=2}^{4} p(k) = 1 \tag{16}$$

as required.

Knowledge of these probabilities allows the number of retardation times in each of the four mechanisms to be expressed in terms of the terminal chain

content of the material. Writing W_k for the number of retardation times associated with mechanism k, we obtain

$$\begin{aligned} W_1(X) &= [D_e(X)][Z(X)] \\ W_2(X) &= [D_e(X)][1 - Z(X)][(1 - X)^2] \\ W_3(X) &= [D_e(X)][1 - Z(X)][2X(1 - X)] \\ W_4(X) &= [D_e(X)][1 - Z(X)][X^2] \end{aligned} \tag{17}$$

where

$$D_e(X) = D_e{}^t/(1 - X)^2 \tag{18}$$

and

$$Z(X) = Z_t(1 - X)^2 \tag{19}$$

To obtain Eq. (18) the expression $(1 - X)^2$, the fraction of trapped entanglements in a blend with terminal chain content X, was substituted for the undetermined function $f(X)$ which appeared in Eq. (13). This is in agreement with the observation of Oberth[21] that the equilibrium moduli of urethane elastomers containing significant amounts of terminal chains decreases by a factor $(1 - v)^2$ where $v(\simeq X)$ is the volume fraction of terminal chains in the network. Substituting Eqs. (18) and (19) into the first two of Eqs. (17) and letting $X \to 0$, we see that Eqs. (17a) and (17b) correctly reduce to $W_1(0) = D_e{}^t Z_t$ and $W_2(0) = D_e{}^t(1 - Z_t)$ for the triblock.

Letting $X \to 1$ in Eqs. (17) through (19) does not lead to equations for the pure diblock because the model is based on the parameters $D_e{}^t$ and Z_t of the triblock, and is thus applicable to blends only. In a blend $X < 1$ always. We shall show later that other considerations require a definite upper limit of X in the model.

Equations (17) to (19) completely determine the change in weighting of the various entanglement mechanisms (i.e. the change in the number of retardation times of unit strength associated with each entanglement mechanism) as the terminal chain content, X, of the blend is varied. The relative importance of each mechanism at a given terminal chain content is expressed most clearly by the ratio $W_k(X)/D_e(X)$, the fraction of the total number of retardation times attributed to each mechanism. These relative weighting factors are plotted against terminal chain content in Figure 3 for mechanisms $k = 2, 3, 4$.

With increasing terminal chain content the relative contribution of trapped entanglements ($k = 2$) decreases monotonically, that of untrapped triblock–diblock entanglements first increases and then decreases, and that of untrapped diblock–diblock entanglements increases monotonically. Thus the relative importance of the kind of entanglement formed changes progressively from mechanism 2 to 3 to 4 as the terminal chain content increases.

Knowing the manner in which the retardation times are distributed among

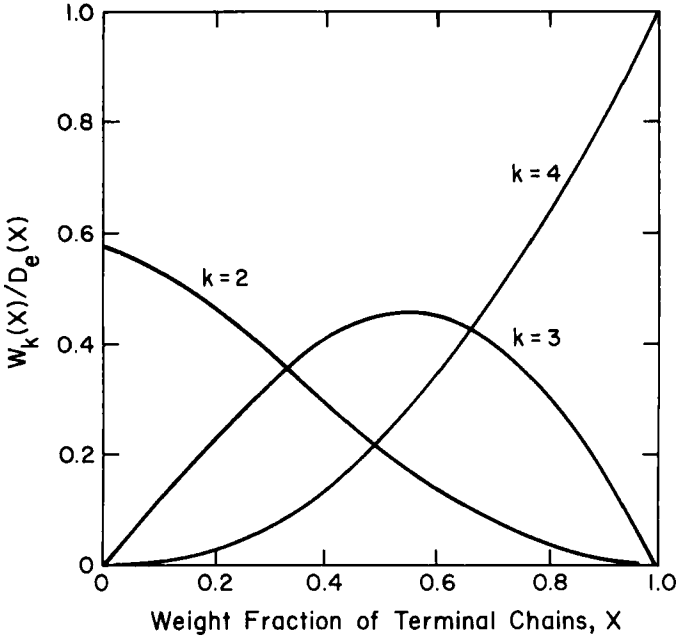

FIGURE 3 Relative weighting factors of the retardation mechanisms $k = 2$, 3, and 4.

the four mechanisms, each D_{ik} value which enters into Eqs. (3) and (4) can be written as

$$D_{ik} = W_k\left(L_{ik}/\sum_{i=1}^{nk} L_{ik}\right) = W_k L_{ik}/A_k \tag{20}$$

for each selected value of τ_{ik}. As in Eqs. (8) and (9), the factor in parentheses gives the normalized value of the strength of the retardation spectrum for the kth mechanism at position τ_{ik} on the time scale. For the triblock, the values of L_{ik} for the two mechanisms contributing to the mechanical behavior could be determined directly from Figure 2. However, at this point the L_{ik}'s and corresponding τ_{ik}'s are unknown for the diblock–triblock blends. Thus, we are confronted with the problem of determining both the location and the shape of the retardation spectra which determine the mechanical response of the blends.

SHAPE AND LOCATION OF THE RETARDATION SPECTRA OF THE BLENDS

Since the shape and location of the transition region is unaffected by terminal chain content,[1,2] the left peak in Figure 2 represents the spectrum of retardation

times associated with mechanism $k = 1$ for all blends. The right peak in Figure 2 is the retardation spectrum associated with the trapped entanglement slippage mechanism ($k = 2$) in the triblock. It is reasonable to expect that the symmetric shape assumed for this peak is preserved when terminal chains are present in the network. However, as discussed earlier, in this case there will be greater distances available for trapped entanglement slippage and this will cause a shift in the location of the spectrum to longer times. The magnitude of this spectral shift will be determined later.

Defining spectral shapes for mechanisms 3 and 4 is difficult because these mechanisms overlap each other and mechanism 2. However, by assuming that the spectra for mechanisms 3 and 4 have the same shape, the shape may be estimated from the data. In Figure 1 the calculated retardation spectra were presented for SBS-8 and for the blend BL-1.3. A reasonable estimate of the left side of the spectral distribution for mechanisms 3 and 4 may be obtained by shifting the peak of the SBS-8 spectrum associated with mechanism 2 (cf. Figure 1) slightly to the right in the manner to be discussed below and then subtracting the ascending branch of the peak from the spectrum of the blends.[12] The descending right side of the spectrum for mechanisms 3 and 4 is assumed to be identical with that of mechanism 2. This rather rough estimate results in a somewhat steeper ascent from the left to the peak value for the spectrum of mechanisms 3 and 4 when compared to the spectrum characterizing mechanism 2.

Figure 4 shows the shapes of the spectra of the blends for mechanisms 1 to 4 plotted on a linear vertical scale. The scale is not shown because the D_{ik} values on which the spectra are based were normalized [cf. Eqs. (12) and (20)] and thus the areas under the curves have no significance. Also, the peak positions have arbitrarily been made to coincide in this figure for easier comparison of the shapes.

We now turn our attention to the locations of the various spectral distributions discussed above. We have anticipated that the spectrum for trapped entanglement slippage will shift to longer times with increased terminal chain content. A rather general prediction of several of the molecular theories for crosslinked and entanglement networks is that the retardation time characteristic of a given viscoelastic mechanism increases in proportion to the square of the length of the chain segment whose motion is associated with that mechanism. For the triblock the segment length which gave rise to the spectral peak for trapped entanglement slippage at $\log \tau = 5.75$ at the reference temperature of $-78°C$ was simply M_e, the average distance between entanglements in our systems. Thus knowledge of the distance between trapped entanglements in a blend with terminal chain content X would allow one to locate the new peak position of the trapped entanglement slippage spectrum by calculating a shift from the original position at $\log \tau = 5.75$. The molecular weight between

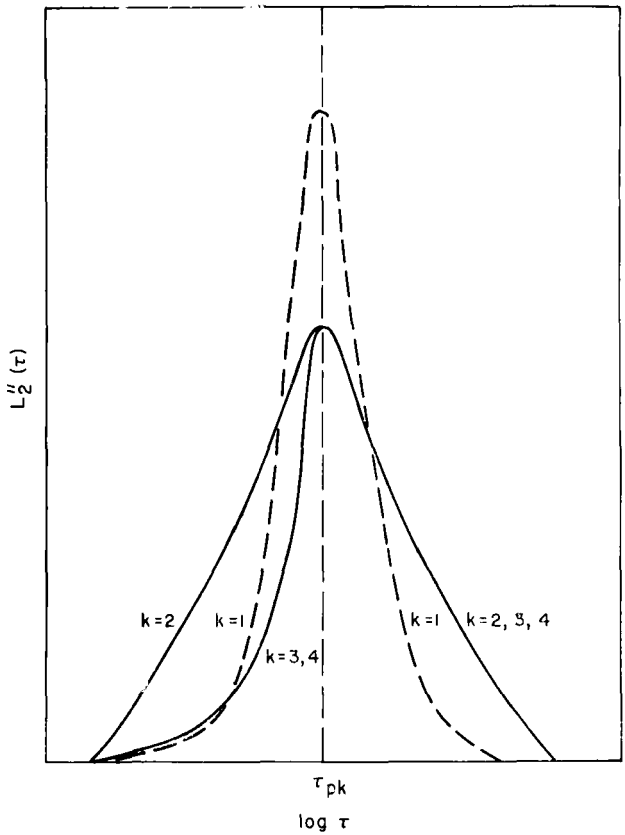

FIGURE 4 Qualitative comparison of the shapes of the retardation spectra for the mechanisms $k = 2$, 3, and 4.

trapped entanglements in a blend, $M_e(X)$, can be found from the expression

$$M_e(X) = M_e N_t / N_2 \tag{21}$$

where N_t is the total number of sites available for trapped entanglements, and N_2 is the number of trapped entanglements in the network.

The probabilities presented in Eq. (15) can be used to evaluate the ratio N_t/N_2. N_2 is clearly proportional to $(1 - X)^2$, the probability of finding a trapped entanglement in the network. N_t should reflect only the probabilities of triblock–triblock and diblock–triblock entanglements, since diblock–diblock junctions do not constitute possible sites for trapped entanglements. Thus N_t incorporates the sum of the first two parts of Eq. (15) and is proportional to $1 - X^2$. The proportionality constant is the total number of entanglements in

each case, and therefore cancels from the expression for $M_e(X)$. The resulting expression for the molecular weight between trapped entanglements in a blend is

$$M_e(X) = M_e(1 + X)/(1 - X) \tag{22}$$

Equation (22) is restricted with respect to the terminal chain content, X. Since M_e is 13,000 for our networks,[1] all values of X greater than 5/7 will predict a molecular weight between trapped entanglements greater than 78,000, the molecular weight of the SBS-8 triblock polybutadiene segments. This is clearly unrealistic, and therefore a critical value of $X = 5/7$ must not be exceeded for the analysis to be meaningful. The value of 5/7 for X_c resulted from the particular values of M and M_e for the system used in this study. In general

$$X_c = \frac{(M/M_e) - 1}{(M/M_e) + 1} \tag{23}$$

The critical terminal chain content marks the point at which there is no longer an average of one trapped entanglement per triblock segment. At this point, large unattached structures would exist within the continuous interconnected block copolymer network, a situation similar to the presence of a sol fraction in conventional elastomers. Thus the model must not be expected to be valid above $X = X_c$.

The location of the spectral peak for mechanism 2 in the blends can now be calculated using Eq. (22). From the known peak location at $\log \tau = 5.75$ for the slippage of polybutadiene segments of molecular weight M_e, Eq. (22), and the dependence of the location on the square of the characteristic slippage length we find

$$\log \tau_{p2} = 5.75 + \log [M_e(X)/M_e]^2 = 5.75 + 2 \log [(1 + X)/(1 - X)] \tag{24}$$

where τ_{p2} represents the location, in the blends, of the peak of the spectrum for mechanism 2, the slippage of trapped entanglements.

Using analogous procedures it is possible to define a characteristic slippage distance for each of the two types of untrapped entanglements. The characteristic length is taken as the average of the distances from the entanglement point in question to the nearest, if any, trapped entanglement along each of the contributing segments.[12] This results in

$$\log \tau_{p3} = 5.75 + 2 \log \left[\frac{M_e(1 + X) - M'(1 - X)}{2M_e(1 - X)}\right] \tag{25}$$

for the location of the peak of the spectrum for mechanism 3, and in

$$\log \tau_{p4} = 5.75 + \log (M'/M_e) \tag{26}$$

for that of mechanism 4.

In Figure 5 Eqs. (24), (25), and (26) are plotted for the particular case of $M' = 51{,}000$ and $M_e = 13{,}000$. At low terminal chain contents the contributions to the longest time response (high values of $\log \tau_{pk}$) arise from untrapped entanglement slippage ($k = 3, 4$). However, as terminal chain content increases, the time-scale of the trapped entanglement slippage mechanism ($k = 2$) increases rapidly until, at high terminal chain contents, this mechanism is responsible for the longest time response of the material.

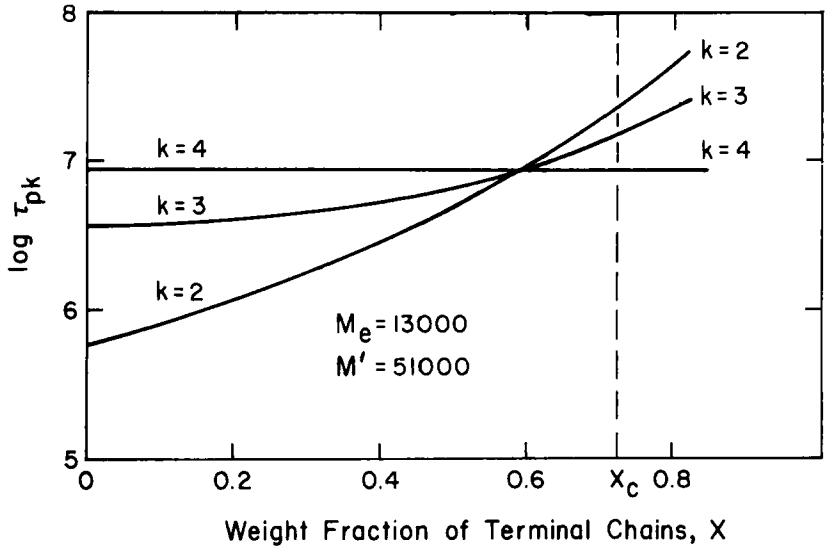

FIGURE 5 Typical variation of the locations of the spectral peaks for mechanisms $k = 2$, 3, and 4.

Equations (24), (25), and (26) define only the peak positions for the spectra associated with mechanisms 2, 3, and 4. The shapes of the spectral distributions around these peaks have already been established as presented in Figure 4. It is reasonable to assume that these shapes will be preserved when the locations of the spectra change. Thus, with Eqs. (24) through (26), and Figure 4, we have fixed both the range of retardation times and their distribution over this range for each of the entanglement slippage mechanisms.

USING THE MODEL

It is now possible to use Eqs. (3) and (4) to generate response curves for materials of varying terminal chain content and length. Equation (17) is used

to calculate the value of W_k for each mechanism. Then, the normalized spectral strength at each value of τ_{ik} is determined from Eq. (20). The τ_{ik} values must be chosen with the range of retardation times appropriate for mechanism k as described by Eqs. (24) through (26). Again, the choice of the spacing of the τ_{ik} values is unimportant as long as they are close enough so that smooth curves are obtained.[12] In practice, a spacing of 0.25 decade was used, resulting in values for n_k of 34 for mechanism 1 and 43 for mechanisms 2 to 4.

Figures 6 to 8 show the comparison between calculated response curves (dashed lines) and those obtained experimentally (solid lines). The network parameters used to calculate the various dashed curves are indicated in the figures. In all figures the curves labeled A refer to the response of the triblock, SBS-8.

It was necessary to cut off the data at the points indicated by the symbols, because, as discussed in the previous papers,[1,2] contributions from the polystyrene phase and the interfacial region complicate the picture at reduced frequencies below the cut-off points. The materials used in the experimental part of this study were thus of somewhat limited value. Clearly a much better study could have been made if a system with no interlayer region and with glassy domains of much higher T_g had been available.

In Figures 7 and 8 several of the calculated curves have no experimental counterpart. They have been included to indicate the wide spread of response predicted by the model.

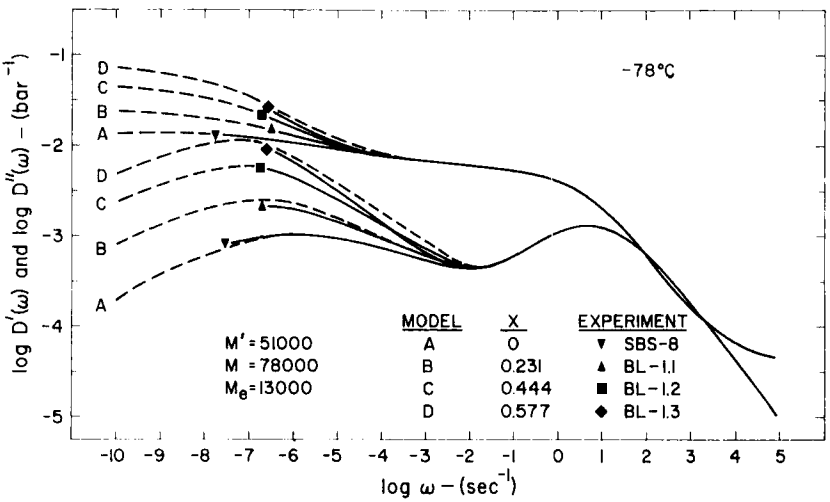

FIGURE 6 Comparison between experimental response curves and the predictions of the model—Series 1.

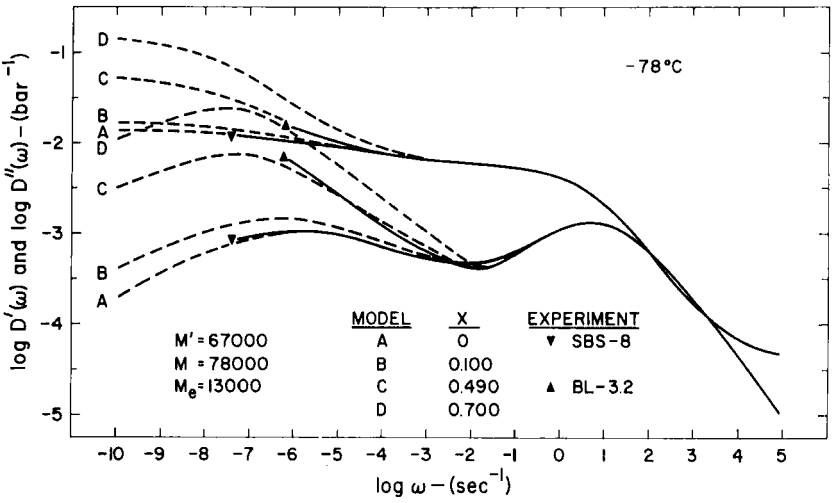

FIGURE 7 Comparison between experimental response curves and the predictions of the model—Series 3.

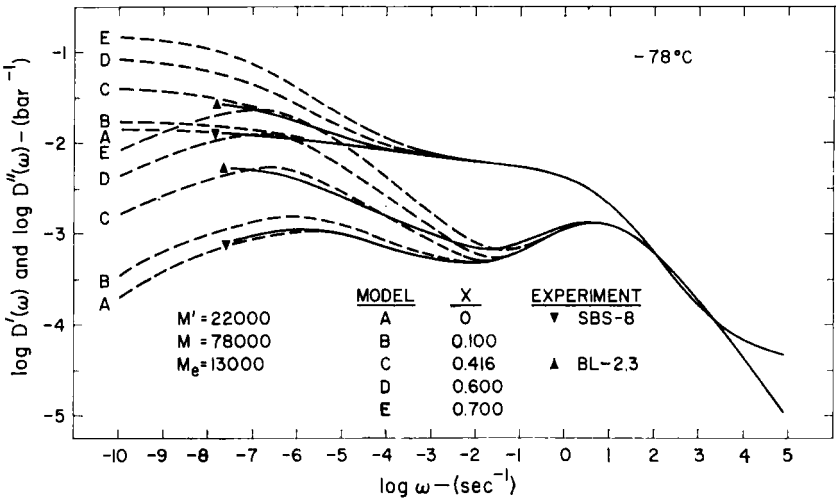

FIGURE 8 Comparison between experimental response curves and the predictions of the model—Series 2.

Figure 6 shows the calculated and observed response curves for the blends containing terminal chains of 51,000 molecular weight. The agreement in the glassy and transition regions is expected since the model has been fitted to the experimental data in that frequency range. At lower frequencies the curves

predicted by the model fan out in substantial agreement with the experimental data. The loss compliances calculated from the model pass through distinct maxima which shift to lower frequencies and higher values as terminal chain content increases. The model predicts storage modulus curves which rise through steeper secondary transitions to attain higher values of D_e with increasing terminal chain content.

Figure 7 shows the comparison for Series 3, containing terminal chains of 67,000 molecular weight. The agreement between the experimental curves and the curves calculated from the model is again very good. The secondary maxima predicted by the model again shift to lower frequencies with increasing amounts of terminal chains. Furthermore, although this is not too clear in the figure, the curves predicted by the model exhibit a deepening minimum near $\log \omega = 2$ as X increases. As proposed in the previous paper,[2] the deepening of the minimum is caused by a downscale shift of the low frequency slippage mechanisms resulting in a reduced contribution to the loss at intermediate frequencies.

Comparisons for Series 2, containing terminal chains of 22,000 molecular weight, are shown in Figure 8. Although the agreement between the calculated response curves and the data are not as good here, the model does correctly predict that the minimum in the loss compliance becomes shallower as the terminal chain content is increased. The shallower minimum is a direct result of the relatively high frequency location of the $k = 4$ mechanism (diblock–diblock entanglement slippage) for Series 2. Since these terminal chains are so short, their contribution appears at high enough frequencies to affect the level of the minimum in the loss compliance. Furthermore, the location of this particular mechanism is independent of X [see Eq. (26)] for a given terminal chain length. Therefore, increasing the terminal chain content raises the level of the minimum by increasing the number of unit strength retardation times in this region. At the same time the secondary peak in the loss curve at lower reduced frequencies still shifts downscale with increased terminal chain content. This is a result of the shift of the $k = 2$ and $k = 3$ mechanisms to longer times as the terminal chain content of the network increases.

SUMMARY AND CONCLUSIONS

The development and use of the model has shown clearly that the low frequency entanglement slippage effects often observed in the mechanical behavior of elastomers arise from the interplay of several overlapping viscoelastic mechanisms. Both the weighting and the location of the contributions from these mechanisms are complicated, yet interrelated, functions of the network composition. It is clear, therefore, that lumping these low frequency

entanglement slippage processes into a single mechanism with a fixed time scale is an oversimplification. Thus, based on the results presented here, it would appear that a model or theory which includes only a single mechanism to account for entanglements in elastomers is likely to lack correlation with the true physical situation.

This analysis has included only the mechanisms of trapped and untrapped entanglement slippage. However, the model could be extended to include the contributions of other structural features, such as motions of covalent crosslink points, if their low frequency retardation mechanisms could be separated and identified. In fact the analysis could be extended to include additional polymer phases. For example, one can visualize introducing mechanisms corresponding to $k = 5$ and $k = 6$ to account for the contributions from the polystyrene phase and from the interlayer. This has not been attempted here. Furthermore, the model completely ignores the temperature dependence of each contributing mechanism, and therefore the overall response predicted by the model is strictly applicable only at a particular reference temperature. However, if one could establish the characteristic temperature dependence of each separate mechanism, the model could conceivably be used to predict the mechanical response at any temperature. In that case the analysis would correspond to an additive compliance model for thermorheologically complex behavior in single phase materials.

The rather good agreement between the calculated curves and experimental data indicates that the model may be useful for estimating the location and the relative importance of the low frequency mechanisms affecting the mechanical behavior of any rubbery material if the concentration and length of the terminal chains in that material are known. At present the model falls short of predicting the overall mechanical response of a conventionally crosslinked elastomer. However, the analysis of entanglement slippage phenomena presented here along with the experimental results presented in the previous papers of this series indicate that fruitful studies can be conducted through the use of model network systems similar to these block copolymer blends. Such studies should add measurably to the understanding of the low frequency viscoelastic mechanisms which influence the observed mechanical behavior of elastomers.

Acknowledgement

This work was supported in part by a grant from the National Science Foundation.

References

1. R. E. Cohen and N. W. Tschoegl, *Intern. J. Polymeric Mater.* **1**, 49 (1972).
2. R. E. Cohen and N. W. Tschoegl, *Intern. J. Polymeric Mater.* **2**, 205 (1973).

3. J. D. Ferry, R. Mancke, E. Maekawa, Y. Oyanagi, and R. Dickie, *J. Phys. Chem.* **68,** 3413 (1964).
4. E. Maekawa, R. Mancke, and J. D. Ferry, *J. Phys. Chem.* **69,** 2811 (1965).
5. R. Dickie and J. D. Ferry, *J. Phys. Chem.* **70,** 2594 (1966).
6. R. Mancke and J. D. Ferry, *Trans. Soc. Rheol.* **12,** 335 (1968).
7. R. Mancke, R. A. Dickie, and J. D. Ferry, *J. Polym. Sci. A*-2, **6,** 1783 (1968).
8. R. H. Valentine, J. D. Ferry, T. Homma, and K. Ninomiya, *J. Polymer Sci. A*-2, **6,** 479 (1968).
9. J. F. Sanders, J. D. Ferry, and R. H. Valentine, *J. Polymer Sci. A*-2, **6,** 967 (1968).
10. N. R. Langley and J. D. Ferry, *Macromolecules* **1,** 353 (1968).
11. J. D. Ferry, *Viscoelastic Properties of Polymers*, 2nd ed., Wiley, N.Y. (1970).
12. R. E. Cohen, Ph.D. Thesis, California Institute of Technology, 1972.
13. A. S. Lodge, *Rheol. Acta*, **1,** 379 (1968).
14. J. D. Ferry, R. F. Landel, and M. L. Williams, *J. Appl. Phys.* **26,** 359 (1955).
15. D. G. Fesko, Ph.D. Thesis, California Institute of Technology, 1971.
16. D.H. Kaelble, *Trans. Soc. Rheol.* **15,** 235, (1971).
17. M. Shen, E. H. Cirlin, and D. H. Kaelble, *Colloidal and Morphological Behavior of Block and Graft Copolymers*, G. E. Molau, ed., Plenum Press, N.Y. (1971).
18. D. G. Fesko and N. W. Tschoegl, *J. Polymer Sci. C*-35, 51 (1971).
19. D. G. Fesko and N. W. Tschoegl, *Intern. J. Polymeric Mater.* **4,** 51 (1974).
20. N. W. Tschoegl, *Rheol. Acta*, **10,** 582 (1971).
21. P. J. Flory, *Industrial and Engineering Chemistry*, **38,** 417 (1946).
22 A. E. Oberth, *Rubber Chem. Tech.* **44,** 152 (1971).